

Episodic reactivation of large-scale push moraines in front of the advancing Taku Glacier, Alaska

E. M. Kuriger,¹ M. Truffer,¹ R. J. Motyka,¹ and A. K. Bucki^{1,2}

Received 2 August 2005; revised 11 October 2005; accepted 31 October 2005; published 14 February 2006.

[1] Taku Glacier, an advancing former tidewater glacier in Alaska, has been actively pushing its proglacial sediments along part of its terminus over the last 50 years, producing so-called push moraines. The mobilization of these sediments, which were locally lifted more than 20 m above sea level by 2004, has happened episodically rather than steadily. The last major event of proglacial sediment deformation occurred in 2001, presumably caused by sliding along a basal detachment layer. Since then, most deformation has been localized within a few meters of the terminus, including impressive deformational features of the terminal ice, where slabs of ice, tens of centimeters in thickness, have undercut proglacial sediments and vegetation and lifted them up. Between 2002 and 2004, surface velocities and horizontal displacements were measured across the terminus and in the proglacial push moraine area. Sediment displacement was highest between the end of March and mid-June. A decrease in displacement with distance from the terminus revealed that the sediments were deforming internally rather than along a basal décollement. We present a simple model which suggests that, under 2004 conditions, reactivation of major movement along this décollement is unlikely to happen, unless some critical factors change. These factors include (1) a steepening of the glacier surface, (2) an increased surface angle of the sediment wedge, and/or (3) higher water pressure in the system, which decreases the effective frictional resistance. An observed wet clay-rich layer presumably acted as a major fault plane during the 2001 event.

Citation: Kuriger, E. M., M. Truffer, R. J. Motyka, and A. K. Bucki (2006), Episodic reactivation of large-scale push moraines in front of the advancing Taku Glacier, Alaska, *J. Geophys. Res.*, *111*, F01009, doi:10.1029/2005JF000385.

1. Introduction

[2] An advancing glacier can, under certain conditions, produce so-called “push moraines,” which are glaciotectionic moraines just below or in front of the glacier terminus. Push moraines display a wide range of different morphologies, at scales from a few meters at the glacier terminus to several hundred meters beyond the advancing ice front. The conditions under which they form are not fully understood and neither are the conditions for continuation or reactivation of push moraine development. This paper deals with an important aspect of the interaction between an advancing glacier and its foreland that has rarely been investigated: the conditions under which a glacier pushes and reactivates existing large-scale deformational bulges in front of its terminus, rather than overriding them.

[3] Glaciotectionic processes play a significant role in a glacier system. *Bennett* [2001] reviewed numerous detailed

geomorphological studies of push moraines from different glaciers in various locations. Most of these studies described ice-marginal sediment deformation [*Humlum*, 1985; *Krüger*, 1985] as well as multicrested push moraines, which extended several hundred meters beyond the glacier terminus [*Croot*, 1987; *Boulton et al.*, 1999]. *Sharp* [1984] and *Krüger* [1993] described deformation at the glacier-sediment interface, which involved both ice and sediments. The only quantitative and very comprehensive study of active push moraines was published by *Kälin* [1971]. The advance of Taku Glacier offers a rare opportunity to collect data on an actively deforming glacier terminus and its foreland.

[4] Push moraines, such as those at Taku Glacier, are mechanically analogous to wedges of soil or snow pushed by a moving bulldozer. A simple model of the process was presented by *Davis et al.* [1983] and *Dahlen* [1984] who used it to examine the deformation of accretionary wedges and propagation of thrust faults on tectonic scales. The resulting “critical taper theory” links the force balance of a sediment pile to its bulk geometry and mechanical properties and to the kinematics of its deformation. *van der Wateren* [1995] and *Fischer and Powell* [1998] applied the critical taper theory to ice-pushed proglacial moraines. Unlike a bulldozer, a glacier is compliant and adapts its

¹Geophysical Institute, University of Alaska Fairbanks, Fairbanks, Alaska, USA.

²Now at ExxonMobil, Houston, Texas, USA.

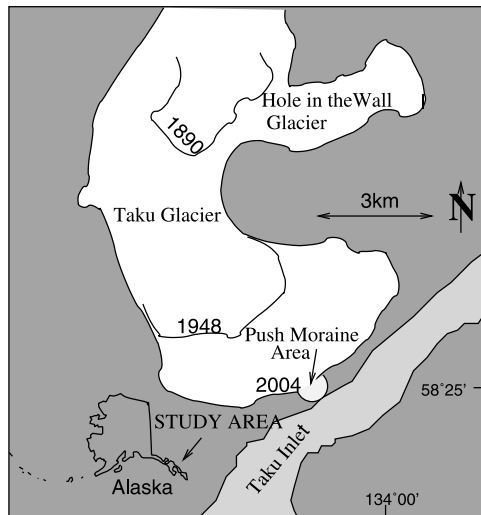


Figure 1. Terminus area of the 60-km-long Taku Glacier. The glacier was advancing in 1890. Until 1948, the glacier was calving into the fjord along its entire terminus. Since then, the area of ice-proximal moraines and uplifted sediments increased continuously and a major push moraine complex developed above sea level at the central part of the terminus.

shape while pushing the sediments beyond the advancing terminus. On a much smaller scale, sandbox experiments reproduced many of the features observed on tectonic scales [e.g., *Mulugeta and Koyi*, 1992; *Lohrmann et al.*, 2003]. Taku Glacier provides a natural laboratory on a larger scale than sandbox experiments and the development of push moraines can be studied within a reasonable time period.

[5] The main research question addressed in this paper is how an advancing ice front interacts with its foreland. Specifically, we investigate why large-scale deformation occurs episodically rather than continuously, and under what conditions this major deformation can be reactivated. In order to answer these questions, we will (1) present a variety of observations of small-scale deformation along the terminus (section 3). Many of these observations have not been previously reported. (2) We present our measurements in the proglacial area (section 4) and (3) use these measurements along with the critical taper theory to explain the episodic deformation of the sediment wedge and to find necessary conditions for future reactivation of large-scale deformation (section 5).

2. Background on Taku Push Moraines

[6] Taku Glacier (700 km², 60 km in length), a temperate, maritime glacier draining the Juneau Icefield, has advanced about 7 km since 1890 into the north end of Taku Inlet (Figure 1) after more than a century of calving retreat [*Motyka and Begét*, 1996]. The present dynamics of Taku Glacier are the result of the tidewater-glacier cycle [*Meier and Post*, 1987] and a large accumulation to total area ratio (AAR) of about 0.90 during the last century [*Post and Motyka*, 1995]. Taku Glacier had a

calving ice front along its entire terminus until 1948, when the shoal terminal moraine was raised above sea level in the central part of the terminus. During subsequent years, ice-proximal moraines developed along most of the face with a dominant deformational push moraine complex in the center. Comparison of aerial photographs from different years has shown that this broad area of proglacial deformation has remained at the same relative position with respect to the terminus since its first appearance in 1948. The development of these moraines plays an important role in the advance of the glacier, as they protect the ice from warm ocean water and thereby prevent ice loss due to calving and submarine melting. The sediment sources for the moraines are primarily remobilized subglacial sediments with additional fluvial contributions from Taku River. Radio echo soundings from 2003 and 2004 [*Kuriger*, 2005, Appendix B] show that the glacier bed forms a trough upglacier of the push moraine complex with a depth of 120 m below sea level at the location of the 1948 shoal moraine. Comparisons with depth soundings by *Nolan et al.* [1995] have shown sediment excavation of $3.7 \pm 0.8 \text{ m a}^{-1}$ between 1989 and 2004 along the centerline of the glacier [*Motyka et al.*, 2005].

[7] A series of aerial photographs taken between 1979 and 1996 revealed an episodic change in shape of the shoal proglacial area. The existence of multiple deformational bulges in the middle part of the terminus was clearly visible by 1979 (NASA, U2-flight, 1979, archived at GeoData Center, Geophysical Institute, University of Alaska Fairbanks, frame number 4259–4260). Their shape changed noticeably by 1989 (U. S. National Ocean Service, 1989, archived at GeoData Center, Geophysical Institute, University of Alaska Fairbanks, frame number A6-175, A6-176) but remained more or less constant over the subsequent years (U.S.D.A. Forest Service, photo acquired by NASA, 1996, archived at Forest Service Information Center, Juneau). In 2001, large-scale sediment deformation was observed and three main bulges (bulge 1 to bulge 3 in Figure 2) and several smaller ones formed up to 200 m in front of the terminus [*Motyka and Echelmeyer*, 2003]. They advanced at an average rate of $9\text{--}15 \text{ cm d}^{-1}$ during the summer. This large movement slowed down by orders of magnitude or ceased completely by September 2001 despite the ongoing terminus advance. Since then, most deformation has occurred within a 5-m-wide section of the terminus or the ice has simply overridden its terminal moraines. Hence movement on two different scales has coexisted since 2001. In addition, some glacier ice advanced over sediments without any signs of moraine formation or sediment deformation.

[8] In this paper we use the term “ice-proximal ridges” for the ice-proximal moraines, which are 1–5 m high sediment piles within 5 m of the terminus. “Proglacial bulges” or just “bulges” refer to the large-scale deformational features up to 200 m beyond the terminus. The general term “push moraine” is defined as: “the product of construction by the deformation of ice, sediment, and/or rock to produce a ridge, or ridges, transverse or oblique to the direction of ice flow in front of, at, or beneath an ice margin,” following the definition by *Bennett* [2001]. All values for elevation are presented in height above ellipsoid

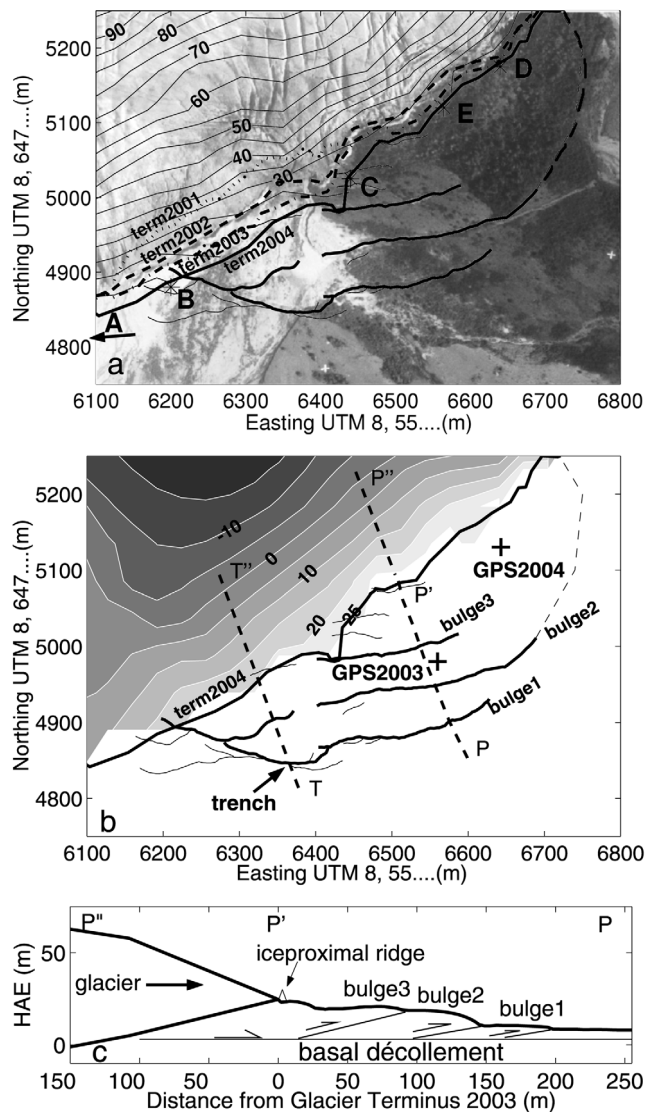


Figure 2. Push moraine area in front of Taku Glacier. (a) Orthophoto 2002 with terminus positions from 2001 to 2004. The contour lines represent the topography of the glacier surface near the terminus (m HAE). The toes of the bulges are shown with solid lines where measured and a dashed line where inferred. Points A–E refer to sites where different deformational features at the glacier-sediment interface were observed (note that A is 400 m west of figure boundary). (b) Map view with the contour lines of the glacier bed (m HAE). GPS2003 and GPS2004 are the locations of continuously running GPS. Arrow labeled “trench” shows the location where a trench was dug, and T-T' and P-P'-P'' show profiles discussed in the text. (c) Cross profile along profile P-P''. The thrust layer at bulge 1 and at the toes of the other bulges was observed. The basal décollement is inferred from seismic refraction measurements (not shown here).

(HAE) which is about 4.1 m higher than geoid height (Geoid99) in our study area.

3. Deformation at the Glacier-Sediment Interface

[9] Ice-proximal ridges were observed during the period of large scale deformation in summer 2001 [Motyka and Echelmeyer, 2003]. They increased in size and/or changed their deformational style by 2004. In addition to the sediments, glacier ice at the very terminus also became incorporated into the deformation. In this section we describe features at five locations (A, B, C, D, E, Figure 2a). They have different characteristics, even though they are only a few hundred meters apart. Descriptions are based on photographs and observations taken in June and August 2003 and 2004. We also present velocity measurements across the ice-proximal ridge at site E. We used precision GPS receivers (TRIMBLE 4000 and TRIMBLE 5700) for position measurements and processed the baselines against a fixed base station situated 100 m in front of bulge 1. The horizontal error in baseline length is about 6 mm.

[10] Site A is located about 400 m west of the area of the proglacial bulges. A roughly 6-m-high and 100-m-long ice-proximal ridge was the dominant feature (Figure 3a). It has caused the advancing glacier to form several 2- to 3-m-thick imbricate thrusts with steep upglacier dipping angles. The glacier outwash in front of the ridge was at an elevation of about 10 m (HAE) and did not show any signs of deformation. This feature was very localized and could not be observed anywhere else along the terminus. The ridge itself was composed of unsorted, well rounded cobbles and boulders, presumably englacially or subglacially remobilized fluvial outwash.

[11] Site B is situated at the very western end of the push moraine area at an elevation of 15 m (HAE). Between 2002 and 2004 the terminus advanced 29 m without any noteworthy deformation of a small secondary bulge (Figure 3b). The advancing glacier was about to override a 1-m-high sediment ridge.

[12] Site C is in an area where the deformation of 2001 raised the proglacial area from about 10 m to 21 m (HAE). The glacier advanced about 28 m between 2002 and 2004. In 2003 and 2004, glacial runoff was abundant and distributed through the area and was flowing either along the terminus or along the toes of small secondary bulges close to the terminus. There were few ice-proximal ridges in this area and none was higher than 0.5 m. We observed that individual ice layers peeled off the underlying or overlying ice. Figure 3c shows a sliver of ice about 10 cm thick that formed a single fold with its axis parallel to the terminus. The lower limb was connected to the glacier; the upper limb was rotated back toward the glacier. We found ice covered by water in front of and below the fold.

[13] Site D, at an elevation of 26 m (HAE), is at a location where an approximately 4-m-deep and 10-m-wide depression separated the push moraine area from the glacier terminus in spring 2003. This depression, located at the eastern end of the area, served as a major water outflow channel from the glacier. The glacier advanced 15 m between 2002 and 2004. By spring 2004 the depression was completely ice filled and sediment ridges, up to 2.5 m high, had formed in front of the terminus and were about to

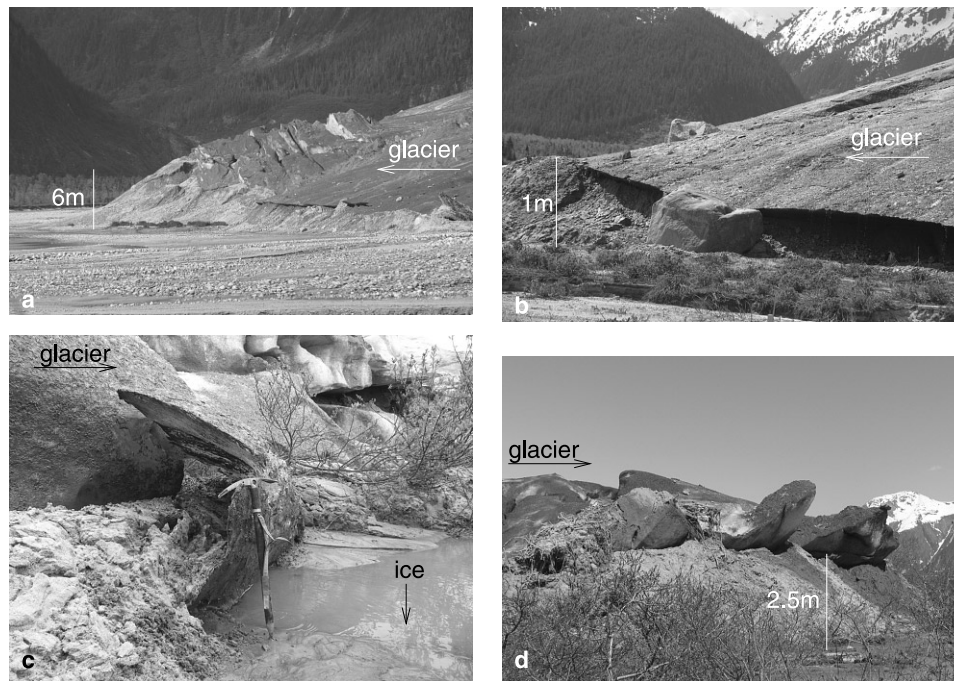


Figure 3. Deformation at the glacier-sediment interface. (a) Site A, 30 August 2004. A 6-m-high sediment ridge causes the advancing ice to form upglacier dipping imbricate thrusts. (b) Site B, 29 May 2004. The glacier overrides the foreland and a 1-m-high sediment ridge. (c) Site C, 11 June 2004. A sliver of ice about 10 cm thick is detached from the subjacent ice (under the water) and folded back toward the glacier. (d) Site D, 15 May 2004. The advancing ice overrides a 2.5-m-high ice-proximal ridge.

be overridden by the advancing ice (Figure 3d). One-meter-thick ice slabs of mainly clear dark ice (i.e., no bubbles, but containing fine dirt) had been pushed over the pile of sediments. A survey marker close to the edge of the glacier moved at a horizontal ice velocity of about 17 cm d^{-1} and a vertical upward velocity of about 1 cm d^{-1} . Within a few meters upglacier from the terminus, the glacier surface became steep and difficult to access.

[14] Site E was characterized by a consistent style but increasing intensity of deformation between 2003 and 2004 (Figure 4). In June 2003 we detected recently torn and uplifted vegetation on a 0.5-m-high sediment ridge. The ridge was ice cored with an about 3-cm-thick slab of ice which was connected to the glacier ice (Figure 4a). Ridges undercut by advancing ice slabs were common along a 100-m-long section around this site. The sediments of the ridge were a composite till (remobilized glacier outwash, subglacial till) without any internal structure. They were composed of boulders and cobbles in sand, silt and clay. In June 2004 the height of the sediment ridge was about 2 m, significantly more than in June 2003. A slab of ice had been pushed up along the ice-proximal part of the ridge (Figure 4b). The mean thickness of this dark clear bubble-free ice was 0.5 m at the slab itself and 0.65 m at the hinge which connected the slab to the glacier at a 90° angle. The ice slab was inclined at a 40° angle at its base and was almost vertical at the top. We measured a mean dip angle of the glacier surface of 35° , which became almost 70° 7 m behind the terminus and decreased to a mean angle of about 17° farther upglacier. During steam drilling for survey markers we hit a 60-cm-thick cavity 5 m behind the terminus where the vertical ice thickness reached 3 m (Figure 4c). A few

meters to the side, a thrust fault had developed within the ice, and no vertical or folded ice slabs were observed. This emphasizes the variability of sediment and ice deformation within short distances of the terminus (Figure 4b).

[15] We placed six survey markers across the proximal ridge at site E, from the glacier ice to the intact vegetation (points 1 to 6 in Figure 4c). Points 1 to 3 were measured over a 4-day interval, point 4 on top of the ice slab twice within 24 hours. The high ablation rate of 10 to 15 cm d^{-1} made more extended measurements of that point difficult. Markers 5 and 6 in front of the sediment pile were surveyed over a 20-day period. Figure 4c summarizes the results. Most of the horizontal compression occurred within 3 m across the sediment ridge (between point 3 and 5), during which the ice between points 1 and 3 was moving as a single block. The vertical upward movement at the top of the ice slab (point 4) was 13.5 cm d^{-1} , similar to the ablation rate at this location. Point 6 did not show any movement on this scale. Between June and August 2004 the crest of the ridge propagated at about 6 cm d^{-1} . Our observations between 2003 and 2004 revealed that underthrusting of the ridge by the advancing ice and subsequent mass wasting at the front of the ridge was the general process of moving the ridge forward rather than bulldozing. Site E was at an elevation of 25 m (HAE) and advanced 24 m between 2002 and 2004.

4. Deformation in the Proglacial Area

4.1. Movement of the Proglacial Bulges

[16] Major movement of the bulges (on the order of cm d^{-1}) ceased by fall 2001 [Motyka and Echelmeyer,

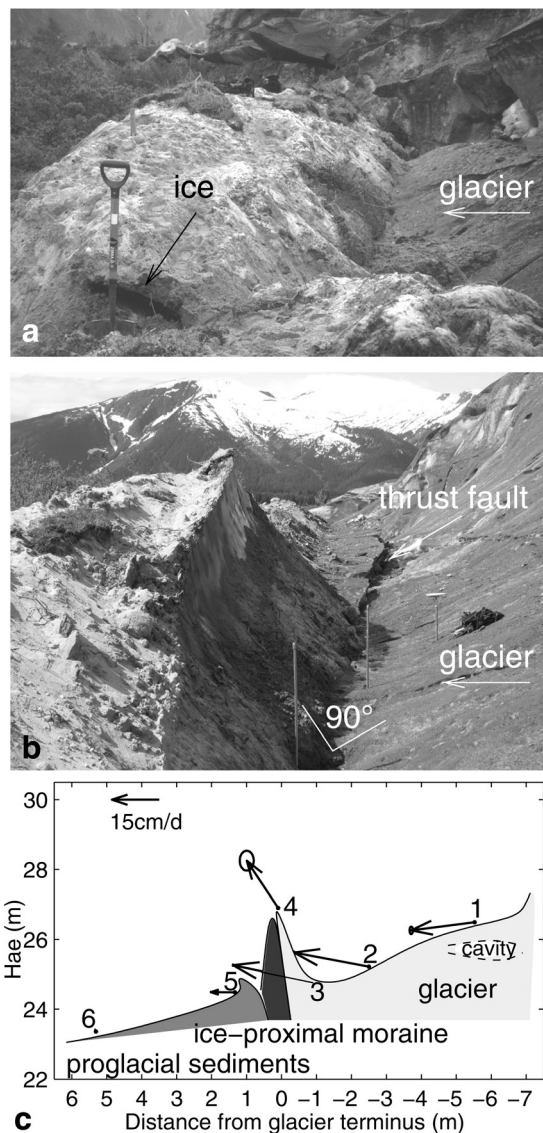


Figure 4. Deformation at the glacier-sediment interface at Site E. (a) 15 June 2003. A 3-cm-thick sliver of advancing ice (appears larger owing to shadows) undercuts vegetation and sediments. (This picture is reversed for clarity.) (b) The same site, 8 June 2004. Ice cored sediment ridge with the ice forming a slab, tens of centimeters thick, that moves almost vertically upward. It is connected to the glacier at an angle of roughly 90° . Several meters to the side, the terminal ice forms thrust faults. (c) velocity cross-profile June 2004. Arrows indicate velocities at different locations with the corresponding error ellipses. A 60-cm-thick cavity was detected below survey marker 1.

2003]. To monitor potential reactivation of movement, we established survey markers along profile P-P' (Figure 2b), which we surveyed biannually between 2002 and 2004 to obtain annual and seasonal variability in horizontal displacement. Displacements were calculated relative to the base station in front of bulge 1. Measurements were made in June and August of the corresponding years. Additionally, a continuously running GPS station on the bulges recorded daily positions between March and August 2003

and between June and August 2004 (GPS2003 and GPS2004 in Figure 2b). The continuous data were analyzed using the GIPSY/OASIS software (version GOA4) developed at the Jet Propulsion Laboratory (JPL) [Zumberge *et al.*, 1997]. We combined data from our sites with data from continuous GPS sites in and around Alaska and estimated daily positions using orbit information provided by JPL (for summary of analysis methods, see Freymueller *et al.* [2000]). The vertical positions in ITRF2000 (International Terrestrial Reference Frame of year 2000) show vertical motions of the site relative to the geocenter, and the horizontal positions in ITRF2000 show the motion of the site relative to a nearby reference site in Whitehorse.

[17] The horizontal displacement along profile P-P' between August 2002 and June 2003 and between August 2002 and August 2003 is shown in Figure 5. The mean direction of the displacements was nearly perpendicular to the glacier terminus. Over the 10-month period the sediments advanced between 15 cm near the terminus and 2 cm at the toe of the outermost bulge 1. The survey point right at the edge of the ice front was displaced 1.36 m, which is more than 10 times the average. This general trend of decreasing displacements with distance from the terminus was also observed over the 1-year period, although the movement of the markers across bulge 1 was irregular. Vertical motion was not detectable within the measurement error.

[18] Velocity calculations along the same profile showed a mean horizontal velocity of about 0.5 mm d^{-1} during summer and 0.2 mm d^{-1} during winter ("summer" refers to the time interval between the beginning of June and the end of August, and "winter" refers to the end of August until the beginning of June).

[19] The continuous measurements of GPS2003 and GPS2004 gave detailed information about the displacement with time. The measurements of GPS2003 (Figure 6a), close to profile P-P', showed a clear onset of horizontal movement by the end of March. The movement was relatively steady until mid-May ($\sim 0.7 \text{ mm d}^{-1}$) and

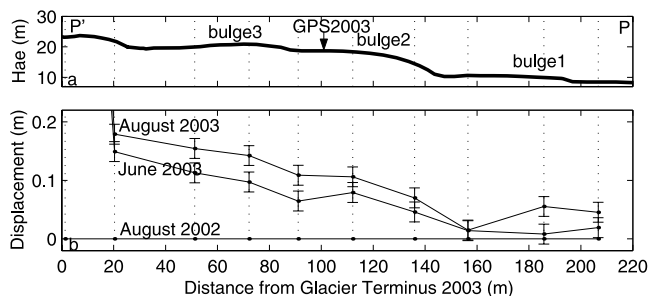


Figure 5. Horizontal displacement along cross-profile P-P' (Figure 2). (a) The topography along the profile is vertically exaggerated. The approximate location of the continuous GPS2003 is indicated by arrow. (b) Horizontal displacement was calculated with respect to August 2002. The middle line shows the displacement after 10 months, and the upper line shows displacement after 1 year. The error range is displayed by vertical lines. The measurement of a survey point 2 m away from the terminus is not plotted, since it was an order of magnitude larger than the others.

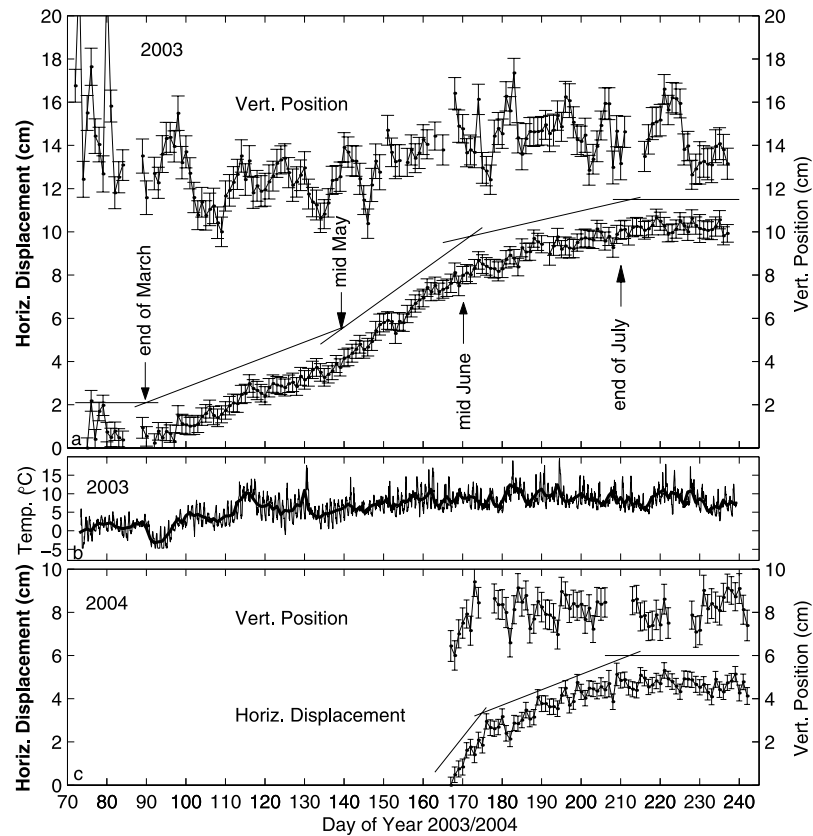


Figure 6. Continuous GPS measurements on the bulges 2003/2004. (a) Daily position measurements on the proglacial bulges at location “GPS2003” and (c) at location “GPS2004”. The upper lines in each figure show the vertical position with respect to an arbitrary point of origin, and the lower lines the horizontal displacement with respect to the first measurement. The corresponding errors are indicated with vertical lines. (b) Air temperature measured close to GPS2003.

increased to $\sim 1.3 \text{ mm d}^{-1}$ until mid-June, followed by a slowdown ($\sim 0.5 \text{ mm d}^{-1}$) and a near complete stop by the end of July. An irregular vertical motion with an amplitude of about 2 cm was detectable throughout the entire period.

A similar pattern both in horizontal and vertical motion was observed at GPS2004 (Figure 6c). However, it was moving at higher rates than GPS2003 (0.8 mm d^{-1} between June and August). GPS2004 was placed closer

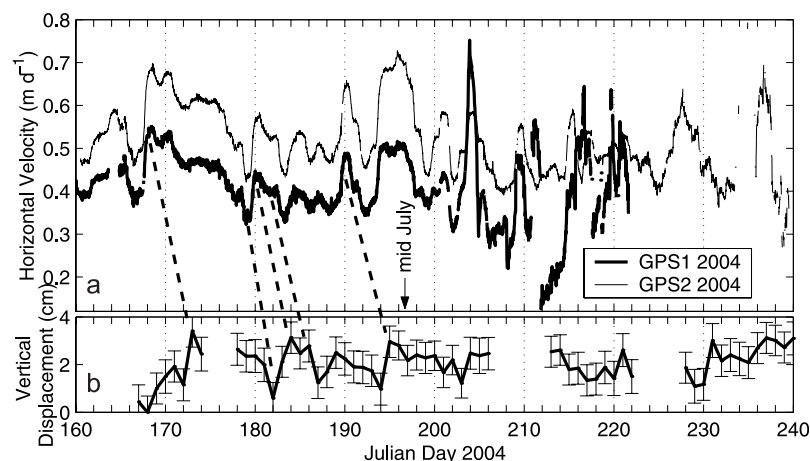


Figure 7. Comparison of daily sediment and ice movement 2004. (a) Daily horizontal velocity at two locations on the glacier surface. “GPS1 2004” was located about 500 m, “GPS2 2004” about 700 m upglacier from the terminus. After day 210 the data became noisier owing to surface ablation and therefore increasingly unstable GPS antennas. (b) Daily vertical position at location “GPS2004” on the proglacial sediments, with respect to an arbitrary point of origin.

Table 1. Sediment Types Within the Trench^a

	Sediment Composition	Thickness	Density	Water Content (by Weight)	Special Characteristics
1	sand/silt with some cobbles	2.7 m	1650 kg m ⁻³	4%	cross-bedding, layers of cobble-free sand
2a	silty clay	0.2 m	1850 kg m ⁻³	35%	laminae: silty clay and silt
2b	clay	0.2–0.5 m		26%	compact
3	sand/silt with clay lenses	2.5 m	1820 kg m ⁻³	19%	
4	silty clay	variable	2005 kg m ⁻³	30%	compact, water rich

^aNumbers in column 1 correspond to Figure 8, where 1 is close to the top of the trench and 4 is close to the bottom of the trench.

to the glacier terminus than GPS2003 and farther to the east, where the glacier was very active in 2004.

[20] During the summers of 2003 and 2004, continuous GPS receivers were also installed on the glacier surface. We calculated daily ice velocities (see Kuriger [2005, Appendix C] for details). The comparison between horizontal ice velocity (Figure 7a) and vertical position of the sediments (Figure 7b) in 2004 showed an almost identical pattern until mid-July, delayed by 3–5 days. Such a correlation was not detected in 2003.

4.2. Internal Structure and Composition of a Bulge

[21] We used a backhoe to dig a trench into the toe of bulge 1, the most distal bulge that formed in 2001 (Figure 2b). In this 9-m-long and 6-m-deep trench we mapped the internal structure using compass and clinometer, determined the sediment composition by estimating the grain sizes in the field, and took sediment samples for which we determined the density and the water content by weighing the samples before and after being dried in an oven.

[22] The results are summarized in Table 1 and Figure 8. The two main sedimentary facies which made up the toe of the bulge were a dry, sand-dominated upper layer including

cobbles (layer 1) and clay-containing layers with higher water contents (layers 2 and 4). This distinction between mud-free and mud-bearing layers could also be made in smaller trenches and bulges eroded by water activity [Motyka and Echelmeyer, 2003]. The presence of water and the increasing instability of the sidewalls made a deeper trench impossible. Free water was observed at the interface between layer 2 (silty clay) and layer 3 (sand/silt) and water accumulated at the bottom of the trench above the compact water-rich clay layer 4.

[23] Three types of thrust surfaces could be distinguished in the walls of the trench: (1) a nearly horizontal 5-m overthrust of sediments onto and over downslope vegetation, (2) an internal thrust with a dip angle of $\gamma = 25^\circ$, inclined toward the glacier, and (3) an imbricate thrust system on a smaller scale (Figure 8). A thin film of silty clay was present along the internal thrust. Assuming that layers 2 and 4 were continuous, the horizontal offset of the internal thrust would result in a displacement of 5 m. On a smaller scale, the imbricate thrust system added a fraction of a meter (Figure 8b) to the shortening. The total horizontal displacement of about 5 m was within the range observed by Motyka and Echelmeyer [2003] in 2001. The uppermost

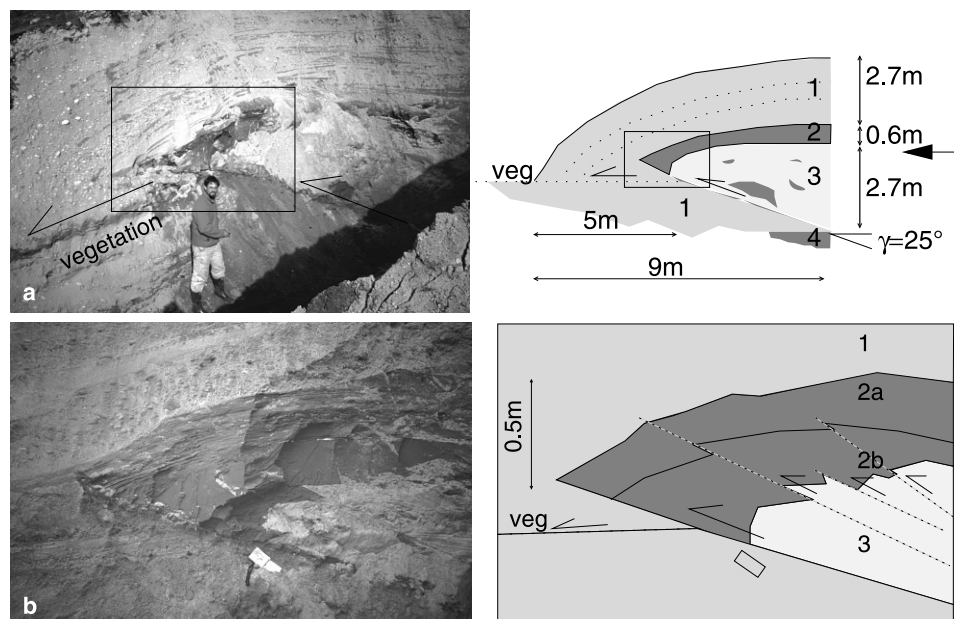


Figure 8. Trench at the toe of bulge 1. The 9-m-long and 6-m-deep trench revealed four sediment layers: sand-silt with cobbles with a low water content (1), laminated silty clay and compact clay with high water contents (2a and 2b), sand-silt with clay lenses (3), and compact silty clay rich in water (4). See Table 1 for details. (a) Primary structural features: a horizontal thrust over the undeformed vegetation and an internal upglacier dipping thrust. (b) Rectangular box from Figure 8a enlarged, showing a fan of imbricate thrusts on a smaller scale. Images were taken on 27 August 2003.

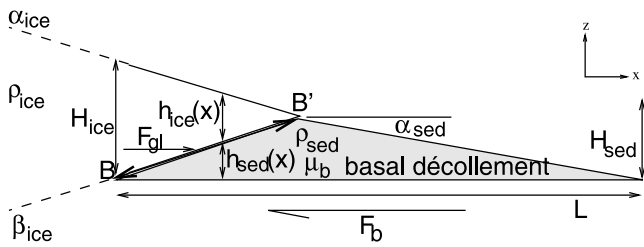


Figure 9. Idealized model of glacier and sediment geometry in the push moraine area used for profiles P-P'' and T-T''. Initiation of movement along the basal décollement happens as soon as $F_{gl} = F_b$. The horizontal glacier force acts along the glacier bed with length $\overline{BB'}$. H_{sed} defines the maximum height of the sediment pile and H_{ice} defines the maximum glacier height, both above the décollement.

sand-silt layer formed an anticline owing to the slip along the vegetation and the internal thrust. Nevertheless, the internal layering was well preserved.

[24] Examination of the trench revealed no evidence of permafrost, such as ice lenses. This is not surprising: All sediments are of marine or glacial origin and were deposited in a temperate marine environment. Even though snow and cold temperatures do occur at sea level in winter, the seasonal cold wave cannot penetrate very far into the sediment and the mean annual temperatures are well above freezing. We will therefore assume that frozen sediments do not play a role in the large-scale deformation described here.

5. Model of Proglacial Bulges

[25] Between 2002 and 2004, ice-proximal deformation and small displacements across the bulges occurred simultaneously. The deformational features along the terminus as well as the strong discontinuity in the horizontal velocity across the ice margin (Figure 4c) were indications that the bulk strain was concentrated within a few meters of the terminus. In contrast to 2001, the force exerted by the glacier was not sufficient to induce plastic deformation in the proglacial sediments. Here we will apply the critical taper theory [Davis *et al.*, 1983; Dahlen, 1984] to find conditions under which either ice-proximal deformation or large-scale movement prevails. With simple considerations we will propose boundary conditions which need to change for a resumption of large-scale movement, as observed in 2001.

[26] An explanation of how glaciotectonic deformation occurs must include two elements: a mechanism enabling the glacier to build up a force which is sufficiently strong to overcome the resistance of the proglacial sediments and/or a mechanism to reduce this resistive force. We will treat this problem by making the following assumptions (Figure 9).

[27] 1. A weak detachment layer exists beneath the proglacial sediments. The importance of a weak layer within the sediments for large push moraine formation was shown by *van der Wateren* [1995]. Seismic refraction measurements in the study area and the presence of water-rich silty clay along the internal thrust within the trench

(which might have been dragged along from a deeper layer during thrusting) provide evidence of a possible basal décollement.

[28] 2. The sedimentary wedge in the push moraine area is at the critical state as defined by *Davis et al.* [1983], where a critically tapered wedge is the thinnest body that can be thrust over its basal décollement without any internal deformation. The critical taper is defined by the sum of the surface slope of the wedge (α_{sed}) and the dip of the basal décollement (β_{sed}), which we take to be $\beta_{sed} = 0$. A subcritical wedge would deform internally and thereby steepen its taper until the critical value is achieved. The geometry and mechanism of the sandbox models from which this theory was derived is similar to what we observe at Taku Glacier.

[29] 3. The sediments are assumed to be homogeneous with a cohesionless Coulomb rheology ($|\sigma_S| = \mu_b \sigma_N$, where σ_S is the shear stress, σ_N the normal stress and μ_b the coefficient of friction at the basal décollement). The effects of anisotropy, for example, due to clay layers within the sand, slightly increase the critical taper but have little effect on the style of deformation [Huiqi *et al.*, 1992]. Also, measurements on sandy materials show the cohesion to be small compared to the normal stress σ_N [Lohrmann *et al.*, 2003].

[30] 4. The glacier profile is wedge shaped with a surface slope α_{ice} and a bed slope β_{ice} .

[31] 5. We treat the problem two dimensionally. In the following, we use the term “force” for force per unit width.

[32] Initiation of movement along the basal décollement happens when $F_{gl} = F_b$. We are only interested in that part of the glacier-sediment system that lies above the basal detachment layer. Therefore F_{gl} is the horizontal glacier force acting along the glacier bed with length $\overline{BB'}$, F_b is the frictional force along the horizontal detachment layer with length L (Figure 9). We applied this model to two longitudinal profiles P-P'' and T-T'' (Figure 2b) extending from the glacier across the push moraines.

5.1. Sediment Strength

[33] The frictional force that resists the motion of the sediments (F_b) is given by the effective normal force on the décollement (F_N) times the coefficient of basal friction μ_b , i.e.,

$$F_b = \mu_b F_N = \int_0^L \mu_b [\sigma_N(x) - p_f] dx, \quad (1)$$

where the normal stress $\sigma_N = \sigma_{zz} = \rho_{ice} g h_{ice}(x) + \rho_{sed} g h_{sed}(x)$. h_{ice} and h_{sed} are ice and sediment height, g is the gravitational acceleration and p_f the pore fluid pressure. By introducing the dimensionless quantity

$$\lambda = \frac{p_f(x)}{\sigma_N(x)}, \quad (2)$$

we can define the pore fluid pressure as percentage of overburden pressure and rewrite equation (1) as

$$F_b = \mu_b F_N = \int_0^L \mu_b [\sigma_N(x)(1 - \lambda)] dx. \quad (3)$$

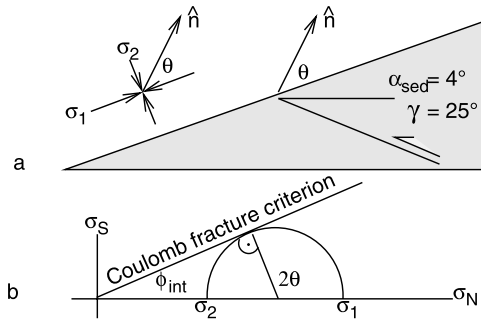


Figure 10. Determination of the angle of internal friction ϕ_{int} . (a) Sketch of the sediment wedge, showing the directions of principle stresses σ_1 , σ_2 , the unit normal \hat{n} to the thrust fault, the dip angle γ of the thrust fault within the trench and the mean surface angle α_{sed} across profile T-T'. (b) Mohr circle to calculate the angle of internal friction ϕ_{int} .

As a first approximation we take λ to equal zero. Applied to the model geometry, equation (1) becomes

$$F_b = \frac{1}{2} \mu_b g H_{\text{sed}}^2 \left[\rho_{\text{sed}} \left(\frac{1}{\tan \alpha_{\text{sed}}} + \frac{1}{\tan \beta_{\text{ice}}} \right) + \rho_{\text{ice}} \left(\frac{\tan \alpha_{\text{ice}} + \tan \beta_{\text{ice}}}{\tan^2 \beta_{\text{ice}}} \right) \right]. \quad (4)$$

Note that the thickness of the glacier H_{ice} is determined by H_{sed} , α_{ice} and β_{ice} .

[34] The inclinations of the glacier surface α_{ice} and glacier bed β_{ice} are determined by linear interpolation between the elevation of the terminus and the measured bed and surface elevations of a point about 50 m upglacier from the margin [Kuriger, 2005, Appendix B]. The wedge slope α_{sed} is the mean inclination between the terminus and the toe of the outermost bulge. We take $\rho_{\text{ice}} = 917 \text{ kg m}^{-3}$ and $\rho_{\text{sed}} = 1800 \text{ kg m}^{-3}$, which is the mean value of the measured densities in the trench (Table 1). Assumptions have to be made for the coefficient of basal friction μ_b and for the depth to the décollement layer in order to determine H_{sed} .

[35] The coefficient μ_b can be estimated with the critical taper theory. The critical taper for a dry wedge and a horizontal basal décollement $\beta_{\text{sed}} = 0$ is given by [Dahlen, 1984] (equation (19) minus equation (9) therein)

$$\alpha_{\text{sed}} = \arcsin \left(\frac{\sin \phi_b}{\sin \phi_{\text{int}}} \right) - \phi_b - \arcsin \left(\frac{\sin \alpha_{\text{sed}}}{\sin \phi_{\text{int}}} \right), \quad (5)$$

where ϕ_{int} and ϕ_b are the angles of internal and basal friction. Again, we use our observations within the trench to determine the coefficient of internal friction $\mu_{\text{int}} = \tan \phi_{\text{int}}$. The main thrust was dipping at an angle of $\gamma = 25^\circ$ (Figure 8) and we assume the principal stress axes to be parallel and perpendicular to the sediment topography in vicinity of the surface (Figure 10a). The angle of internal friction $\phi_{\text{int}} = 2\theta - \frac{\pi}{2}$ is determined through the Mohr circle (Figure 10b), where $\theta = \frac{\pi}{2} - \alpha_{\text{sed}} - \gamma$. This results in $\phi_{\text{int}} = 32^\circ$ or $\mu_{\text{int}} = \tan \phi_{\text{int}} = 0.6$. These values are in the general range for granular materials and were also measured by Lohrmann *et al.* [2003] in sandbox experi-

ments. Together with $\alpha_{\text{sed}} = 4^\circ$, the mean surface angle across the trench profile T-T', equation (5) leads to a coefficient of basal friction $\mu_b = \tan \phi_b = 0.2$. This is within the range of values determined by Bowles [1984] for soils with more than 60% clay fractions. The Taku push moraines with mean surface angles of 4° – 5° agree with observations in sandbox models, where glide horizons with low basal friction support wedges with narrow tapers.

[36] A simple geometrical analysis yields the location of the décollement at 3 m HAE: In a cross section, a rectangular area of sediments removed by shortening must equal that of the triangular pile accumulated in front of the pushing glacier. We know the present length and surface slope of the sediment wedge along profile T-T', and the distance the glacier advanced since 1996 (from the aerial photograph taken in 1996 when this area was still a flat outwash plane). Preliminary results of seismic refraction work in the proglacial area also delineated a strong interface at about the same depth across a broad area of our study site.

5.2. Horizontal Glacier Force

[37] We separate the horizontal longitudinal glacier stress into two parts, a lithostatic stress due to overburden pressure $\rho_{\text{ice}} g h_{\text{ice}}$ and a tectonic stress due to longitudinal compression or extension σ_{xx}^t . The lithostatic stress increases proportionately with depth and the tectonic stress is assumed to be constant with depth. Therefore the glacier force that acts on an imaginary vertical wall at the location where the basal detachment layer intersects the glacier bed (Figure 9) becomes

$$F_{gl} = \int_0^{H_{\text{ice}}} [\rho_{\text{ice}} g h_{\text{ice}}(z) + \sigma_{\text{xx}}^t] dz = \frac{1}{2} \rho_{\text{ice}} g H_{\text{ice}}^2 + \sigma_{\text{xx}}^t H_{\text{ice}}. \quad (6)$$

We used survey markers on the ice surface along profile P-P', which were measured at the end of August 2003, the beginning of June 2004 and the end of August 2004, to calculate the horizontal strain rate $\dot{\epsilon}_{\text{xx}}$ in the flow direction for winter and summer. Then, we determined the tectonic stress contribution σ_{xx}^t by inverting Glen's flow law for ice [Glen, 1955]. For a simple estimate we equated the effective strain rate $\dot{\epsilon}_{\text{eff}}$ with $\dot{\epsilon}_{\text{xx}}$, ignoring contributions from

Table 2. Resistive Sediment Force F_b Versus Applied Glacier Force F_{gl} for Cross Profiles T-T' and P-P'^a

	Profile T-T'	Profile P-P'
	<i>Sediments</i>	
F_b	14.9 MN m ⁻¹	20.4 MN m ⁻¹
α_{sed}	4°	5°
H_{sed}	18 m	21.5 m
μ_b	0.2	0.2
	<i>Glacier</i>	
F_{gl} (summer)	8.44 MN m ⁻¹	18.3 MN m ⁻¹
F_{gl} (winter)	9.44 MN m ⁻¹	19.3 MN m ⁻¹
F_{liith}	6.44 MN m ⁻¹	15.5 MN m ⁻¹
F_{tect} (summer)	2.0 MN m ⁻¹	2.8 MN m ⁻¹
F_{tect} (winter)	3.0 MN m ⁻¹	3.8 MN m ⁻¹
α_{ice}	11°	17°
β_{ice}	10°	10°

^aSee Figure 2.

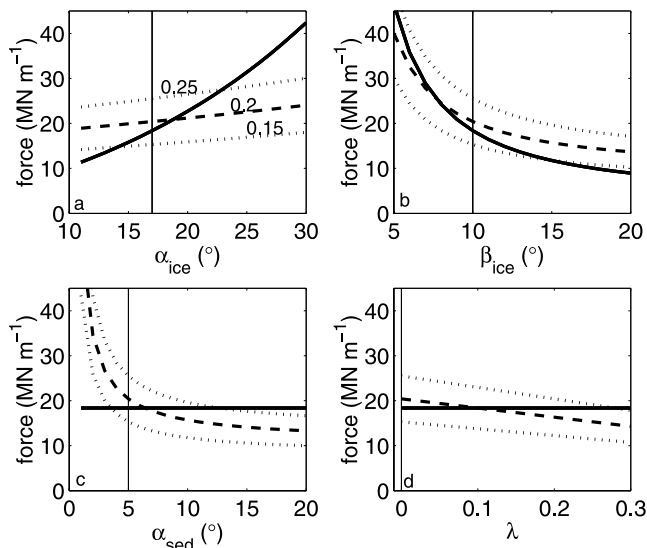


Figure 11. Sensitivity analysis profile P-P''. Sensitivity of the resistive sediment force (dashed lines) and applied glacier force (solid lines) with respect to the parameters (a) α_{ice} , (b) β_{ice} , (c) α_{sed} , and (d) λ along profile P-P''. The vertical lines mark the parameter values found for the 2004 geometry or, in Figure 11d, the assumptions made in our model. Dotted lines show the sediment force calculated with a higher or lower coefficient of basal friction μ_b than the one resulting from the critical taper theory. Points where the solid and dashed/dotted lines intersect provide values of the corresponding parameter necessary to initiate basal movement.

other stress components. The inverted Glen's flow law becomes

$$\sigma'_{xx} = A^{-1/n} \epsilon_{eff}^{1-n} \epsilon_{xx} \approx A^{-1/n} \epsilon_{xx}^{1/n}, \quad (7)$$

with $n = 3$ and the rate factor $A = 0.1 \text{ a}^{-1} \text{ bar}^{-3}$ [Truffer *et al.*, 2001, and references therein].

5.3. Results and Sensitivity Analysis

[38] The results of the force calculations are listed in Table 2. The measured geometries for both profiles result in glacier forces that are too small to overcome the resistive forces along the décollement. The glacier force is larger during winter due to a larger tectonic contribution. Critical controls that may change in order to reactivate large-scale movement along the basal décollement are (1) the glacier profile, (2) the taper of the sediment wedge, and/or (3) the effective basal friction. By introducing the term "effective basal friction" we point out that the influence of pore water in the system should not be neglected as stated in the assumptions for our model. *Hubbert and Rubey* [1959] demonstrated that the critical shear stress along a thrust plane is reduced by pore fluid pressure p_f (equation (1)).

[39] The water content of the sediments (Table 1) shows that the sediments are not fully water saturated although water-rich layers do exist. Also, the presence of free water between layers and the abundance of water along the toes of some bulges shows that water must flow along distinct layers within the sediments. Pore fluid pressure can be enhanced either by compaction of impermeable strata (such

as the clay layer observed in the trench) or transmission of water into a confined aquifer.

[40] We computed the influence of changing boundary conditions α_{ice} , β_{ice} , α_{sed} and the parameter λ , the ratio between pore fluid pressure p_f and overburden pressure. We changed one of these parameters while holding the others at a fixed value (equations (3), (4) and (6)). Because the coefficient of basal friction μ_b was estimated, we also calculated the influence of different values of μ_b on the resistive sediment force. The results are presented in Figure 11 for profile P-P'' and Figure 12 for T-T''. They show that a steepening of the glacier topography α_{ice} , a decrease in the steepness of the glacier bed β_{ice} , a steeper sediment wedge α_{sed} and the existence of water within the sediments are ways to mobilize the sediments along the basal décollement.

6. Discussion

[41] The interaction of the advancing ice with its foreland took various forms: (1) the glacier overrode the proglacial area independent of the presence of a sediment pile against which the glacier could buttress (Sites B and D, Figures 3b and 3d), (2) ice and/or ice-proximal sediment ridges deformed within a few meters of the terminus (Sites A, C, E, Figures 3a, 3c and 4) and (3) sediment movement occurred 200 m beyond the terminus (Figure 5). An explanation for these behaviors can be given with the simple model presented above. It showed that in 2004 glacier and sediment did not show a geometry favorable for mobilization of the sediment wedge along a basal detachment layer. We will now discuss the changes that are most likely to lead to a critical change in the glacier or sediment force and thereby determine the future development of the proglacial area of Taku Glacier.

6.1. Model Interpretation

[42] With the calculated $\mu_b = 0.2$ a steepening of the glacier topography α_{ice} is the most efficient way to mobilize the sediments along the basal layer (Figure 11a). Along

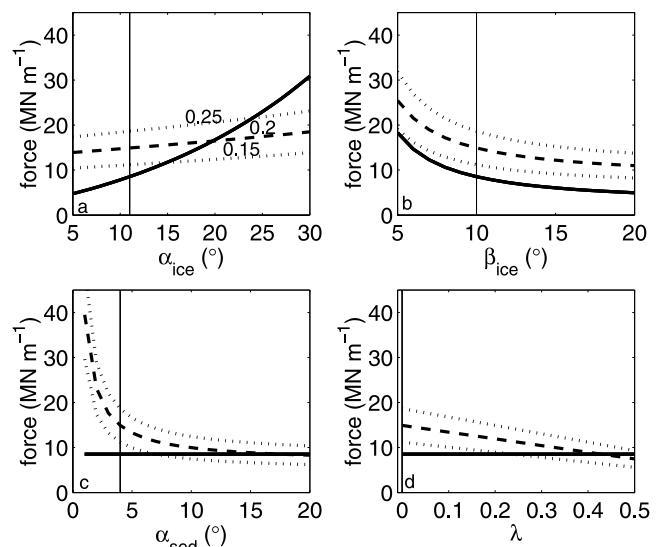


Figure 12. Same as Figure 11, but for sensitivity analysis profile T-T''.

profile P-P'', α_{ice} needs to increase from 17° to 19°. This is more likely to happen than an increase from 11° to 20° along T-T'' (Figure 12a). Digital elevation models which were created from aerial photographs taken in 2002 and 2003 in the terminal area show an increase of α_{ice} along P'-P'' of about 2° to 3°. In addition, our observations of the deformational features along the glacier-sediment interface and the large velocity gradient across the ice-proximal ridge demonstrated that active deformation of terminal ice took place. At site D, for example, the glacier was actively steepening its surface between 2002 and 2004. It is noteworthy that an increased terminus advance does not necessarily imply surface steepening. We have observed much less ice-proximal deformation at locations with higher advance rates and a lower elevation of the terminus (site B, Figure 3b).

[43] Under the assumptions of our model an increase in the steepness of the glacier bed β_{ice} results in a lower glacier to sediment force ratio (Figure 11b). This does not coincide with the observation that the present push moraines developed in an area where a deep trough of the glacier bed had formed upglacier from the terminus. The glacier might transmit stresses from farther upglacier than we assumed in our model and this stress transmission might be favored by steep glacier beds. Additionally, α_{ice} and β_{ice} can not be treated as independent parameters. The model presented here is too simple to address this question and a flow model that couples α_{ice} and β_{ice} would be necessary.

[44] Steepening of the sediment wedge lowers the resistive sediment force (Figure 11c), because of a shorter contact on the detachment layer. In our model, an increase of α_{sed} from 5° to 6° along profile P-P'' is needed. With the current advance rate of the glacier terminus on the order of 10 m a⁻¹ and under the assumption of a constant elevation of the terminus, the sediment wedge would achieve this taper within the next 4 years. This statement is not true along profile T-T'' (Figure 12c), where an increase of α_{sed} from 4° to 16° would be necessary. However, the critical taper equation (equation (5)) relates an increase of the critical taper at a fixed basal friction to a decrease in internal friction. The sediment wedge might be at a subcritical state and the ongoing slow movement of the proglacial bulges might be due to internal deformation. The decreasing displacement with distance from the terminus supports this conclusion.

[45] The assumption of drained sediments with zero pore fluid pressure is clearly an oversimplification. The effect of water flow in the sediments is twofold: the presence of water leads to an effective pressure (and a nonzero λ in equation (2)), and the hydraulic gradient leads to a seepage force that counteracts the gravitational body force. The first effect can be investigated by testing the model sensitivity to changes in λ . It shows that a pore fluid pressure of 10% of the overburden pressure at P-P'' and 40% at T-T'' (Figures 11d and 12d) would initiate movement. Quantifying the second effect would require a more detailed knowledge of the hydraulic regime. Most of Taku's runoff is concentrated in a series of outlet streams along the glacier terminus. Upward seepage should be expected in the proglacial area [e.g., Boulton and Caban, 1995], even without permafrost in the proglacial area. The sediments in front of Taku Glacier are very inhomogeneous, consisting of permeable

sands and very low permeability clay layers, some of which are tilted (Figure 2c). Water is indeed observed to upwell at a few discrete locations along the toes of the various bulges. This inhomogeneous water flow constitutes perhaps the largest uncertainty in the discussion of the force balance. A detailed investigation of the proglacial hydrology would be necessary to address this properly.

[46] The sensitivity calculations show that reactivation of large scale deformation is more likely to happen in the area of profile P-P'' (Figure 11) than profile T-T'' (Figure 12). At profile P-P'', a lower coefficient of basal friction μ_b than we calculated would enable slip along the basal layer under the 2004 geometry (Figure 11). Variability of sediment composition, changing décollement depth or variable water input within the area were not taken into account.

[47] The critical taper theory assumes constant frictional properties. *Mulugeta and Koyi* [1992] observed episodic events in their sandbox experiments, even with constant forcing by a steadily moving backwall. They related the episodic material accretion in sandbox experiments to a stick-slip mode of the décollement propagation. Figure 1 in their paper shows a similarity to the push moraine area in front of Taku Glacier despite different boundary conditions. The advancing glacier does not move steadily and its pushing front is not a rigid vertical wall. However, the similarity of the observations suggests that frictional behavior might be more important than the geometry of the system. Stick-slip mode and its applicability on tectonic scales for fault reactivation during earthquakes was also described by *Marone* [1998]. *Lohrmann et al.* [2003] showed that sand exhibits a frictional behavior with strain hardening prior to failure and subsequent softening until the onset of stable movement at constant friction. We ignored such effects in our model for the Taku push moraines and might have underestimated the frictional strength. However, once the movement is initiated, a lower stable friction facilitates major events.

6.2. Continuous GPS Interpretation

[48] Our results from the continuously running GPS stations on the sediments have shown an increased velocity between the end of March and the end of July (Figure 6a), a time that coincides with higher water input from the glacier. A spring speed up in horizontal motion beginning in April was also observed on daily ice surface velocities [*Kuriger*, 2005, Appendix D], which we relate to increased water pressure at the glacier bed. We attribute the onset of horizontal movement of the continuous sediment station GPS2003 to increasing water input into the glacier-sediment system, which was caused by an increase of the mean daily air temperature from around 0°C to 7°C during April (Figure 6b). The slowdown of the horizontal sediment movement by mid-June and the complete stop by the end of July as seen in 2003 and 2004 happened despite the abundance of water in the proglacial area until late August. This is quite similar to daily ice velocity observations, where the establishment of good hydraulic connections leads to lower water pressures and storage [*Paterson*, 1994]. A similar mechanism might be operating in the proglacial sediments. The correlation between horizontal glacier velocity and vertical sediment position as observed in 2004 also ceased by late July (Figure 7). We interpret the

delay of 3–5 days between ice velocity and vertical sediment position as the reaction time the water needs to penetrate through the sediments and increase the pore fluid pressure p_f . On the other hand, we do not have a satisfactory explanation for the almost exact match of the curve shape for such a large time lag. One would expect damping of the high-frequency signals due to diffusion of water through the sediments. Also, the assumption of water pressure diffusion is in direct contrast with the $\lambda = 0$ assumption of the force balance. This is again an indication that we do not understand the hydrological system well enough, as already discussed above.

[49] Larger displacements in our cross-profile P-P' during the summer month (Figure 5), the fact that the 2001 movement was observed during late spring and summer [Motyka and Echelmeyer, 2003], and the presence of water along the internal thrust in the trench are arguments for the importance of water. In addition, our estimation of the tectonic contribution to the applied glacier force is larger during the winter months (Table 2) which extend into June. The 2003 continuous GPS data on the glacier surface [Kuriger, 2005, Appendix D] indicate compression into June and plug sliding afterwards. Together with an increased water pressure, the tectonic stress could have been important for the onset of sediment movement by the end of March.

7. Conclusions

[50] Taku Glacier, previously a tidewater glacier, has built its terminal shoal moraine over the last 50 years. The ongoing advance has produced a series of proglacial bulges due to glaciotectonic processes. Comparison of aerial photographs and recent investigations have shown that, despite a continuous terminus advance, sediment movement is determined by few major episodic events rather than steady deformation of the glacial forefield. Several explanations for this behavior can be drawn from this study.

[51] 1. Under 2004 conditions, the applied glacier force cannot overcome the resistive force of the proglacial sediments. This is indicated by large ice deformation along the ice-sediment interface and a large velocity gradient across ice-proximal ridges. Overriding glacier ice at other locations supports this conclusion.

[52] 2. Steepening of the glacier surface is the most effective way to increase the force exerted by the glacier.

[53] 3. Enhanced sediment motion during summer, a time when water is abundant, indicates that decreased frictional resistance by infiltration of water into the system is important. Increased pore fluid pressure might play a key role in sediment movement. A detailed treatment of sediment hydrology was not possible in this study; this constitutes perhaps the largest uncertainty in the force balance calculations.

[54] 4. Between 2002 and 2004 the proglacial sediments were not at the critical taper and the wedge deformed internally with the magnitude of the deformation increasing toward the terminus. The sediment wedge must shorten, and thereby increase its surface slope, to reduce the sediment strength with respect to the force of the glacier. This could happen within as little as 4 years.

[55] 5. Episodic movement of the sediment wedge is related to a critical combination of several boundary conditions including inclination of the glacier surface, surface slope of the sediment wedge and pore fluid pressure within the sediments. Comparison with sandbox models shows that changing frictional conditions are a possible reason for such movements and that episodic movement is possible under steady forcing.

[56] 6. Our calculations for the glacier force involve assumptions that might be oversimplifications, because the influence of the inclination of the glacier bed does not coincide with our observations. Analyses for stress transmission within the ice and along the glacier bed may be essential. A more sophisticated model of the whole system requires a better model of the proglacial sediments.

[57] 7. Currently, we do not have a good understanding of the evolution of the ice-sediment geometry, i.e., the interdependence of β_{ice} and α_{ice} . This depends on processes such as sediment excavation, which are possibly related to freeze-on and routing of subglacial water.

[58] A continued ice supply to the terminus of Taku Glacier can either lead to a steepening of the glacier surface or a shortening of the proglacial taper. The former would increase the force that the glacier exerts on the sediments and the latter can lead to a reduction of the force necessary to induce large-scale formation. In the meantime, ice-proximal deformation will prevail. If the hydrological system of the sediment indeed undergoes seasonal changes as hypothesized, we would expect initiation of large-scale deformation in early spring when water becomes available, but no effective drainage systems are established. This would be quite similar to what is observed for glaciers [e.g., Fountain and Walder, 1998].

[59] **Acknowledgments.** This study was supported by U.S. National Science Foundation, grant OPP-0221307. Field equipment was provided by UNAVCO and VECO Polar Resources. Free flights to the study site were sponsored by ERA helicopters. We would like to thank J. M. Amundson, E. S. Boyce, M. P. Lüthi, and S. O'Neil for their help in the field, and J. T. Freymueller for his assistance with the continuous GPS analysis. K. A. Echelmeyer, W. D. Harrison, and L. H. Shapiro made significant improvements to the manuscript. We appreciate the efforts of the Associate Editor, Neal Iverson, and the two reviewers, Martin Sharp and Matthew Bennett, whose insightful comments helped improve the manuscript.

References

- Bennett, M. R. (2001), The morphology, structural evolution and significance of push moraines, *Earth Sci. Rev.*, *53*, 197–236.
- Boulton, G. S., and P. Caban (1995), Groundwater flow beneath ice sheets: Part II. Its impact on glacier tectonic structures and moraine formation, *Quat. Sci. Rev.*, *14*, 563–587.
- Boulton, G. S., J. J. van der Meer, D. J. Beets, J. K. Hart, and G. H. J. Ruegg (1999), The sedimentary and structural evolution of a recent push moraine complex: Holmstrombreen, *Spitsbergen, Quat. Sci. Rev.*, *18*, 339–371.
- Bowles, J. E. (1984), *Physical and Geotechnical Properties of Soils*, second ed., McGraw-Hill, New York.
- Croot, D. G. (1987), Glacio-tectonic structures: A mesoscale model of thin-skinned thrust sheets?, *J. Struct. Geol.*, *9*, 797–808.
- Dahlen, F. A. (1984), Noncohesive critical Coulomb wedges: An exact solution, *J. Geophys. Res.*, *89*(B12), 10,125–10,133.
- Davis, D., J. Suppe, and F. A. Dahlen (1983), Mechanics of fold-and-thrust belts and accretionary wedges, *J. Geophys. Res.*, *88*(B2), 1153–1172.
- Fischer, M. P., and R. D. Powell (1998), A simple model for the influence of push-moraine banks on the calving and stability of glacial tidewater termini, *J. Glaciol.*, *44*(146), 31–41.
- Fountain, A., and J. Walder (1998), Water flow through temperate glaciers, *Rev. Geophys.*, *36*(3), 299–328.

- Freyemueller, J. T., S. C. Cohen, and H. J. Fletcher (2000), Spatial variations in present-day deformation, Kenai Peninsula, Alaska, and their implications, *J. Geophys. Res.*, *105*(B4), 8079–8101.
- Glen, J. W. (1955), The creep of polycrystalline ice, *Proc. R. Soc. London, Ser. A*, *228*(1175), 519–538.
- Hubbert, M. K., and W. M. Rubey (1959), Role of fluid pressure in mechanics of thrust faulting: I. Mechanics of fluid-filled porous solids and its application to overthrust faulting, *Geol. Soc. Am. Bull.*, *70*, 115–166.
- Huq, L., K. R. McClay, and D. Powell (1992), Physical models of thrust wedges, in *Thrust Tectonics*, edited by K. R. McClay, pp. 71–81, CRC Press, Boca Raton, Fla.
- Humlum, O. (1985), Genesis of an imbricate push moraine, Höfdabrekkujökull, Iceland, *J. Geol.*, *93*(2), 185–195.
- Kälin, M. (1971), The active push moraine of the Thompson Glacier, Axel Heiberg Island, Canadian Arctic Archipelago, Ph.D. thesis, Swiss Fed. Inst. of Technol. ETH, 68 pp., Zurich, Switzerland.
- Krüger, J. (1985), Formation of a push moraine at the margin of Höfdabrekkujökull, south Iceland, *Geogr. Ann., Ser. A*, *67*(3–4), 199–212.
- Krüger, J. (1993), Moraine-ridge formation along a stationary ice front in Iceland, *Boreas*, *22*, 101–109.
- Kuriger, E. M. (2005), Terminus dynamics and deformation of proglacial sediments at the advancing Taku Glacier, Alaska, U.S.A., Master's thesis, Univ. of Alaska Fairbanks, Fairbanks.
- Lohrmann, J., N. Kukowski, J. Adam, and O. Oncken (2003), The impact of analogue material properties on the geometry, kinematics, and dynamics of convergent sand wedges, *J. Struct. Geol.*, *25*, 1691–1711.
- Marone, C. J. (1998), Laboratory-derived friction laws and their application to seismic faulting, *Annu. Rev. Earth Planet Sci.*, *26*, 643–696.
- Meier, M. F., and A. Post (1987), Fast tidewater glaciers, *J. Geophys. Res.*, *92*(B9), 9051–9058.
- Motyka, R. J., and J. E. Begét (1996), Taku Glacier, southeast Alaska, U.S.A.: Late Holocene history of a tidewater glacier, *Arct. Alp. Res.*, *28*(1), 42–51.
- Motyka, R. J., and K. A. Echelmeyer (2003), Taku Glacier (Alaska, U.S.A.) on the move again: Active deformation of proglacial sediments, *J. Glaciol.*, *49*(164), 50–58.
- Motyka, R., E. Kuriger, and M. Truffer (2005), Excavation of sediments by tidewater glacier advance and implications for the oceanic sediment record, Taku Glacier, Alaska, USA (abstract), paper presented at Spring Meeting 2005, Eur. Geosci. Union, Vienna.
- Mulugeta, G., and H. Koyi (1992), Episodic accretion and strain partitioning in a model sand wedge, *Tectonophysics*, *202*(2–4), 319–333.
- Nolan, M., R. J. Motyka, K. A. Echelmeyer, and D. C. Trabant (1995), Ice-thickness measurements of Taku Glacier, Alaska, USA, and their relevance to its recent behavior, *J. Glaciol.*, *41*(139), 541–553.
- Paterson, W. S. B. (1994), *The Physics of Glaciers*, third ed., 481 pp., Elsevier, New York.
- Post, A., and R. J. Motyka (1995), Taku and LeConte Glaciers, Alaska: Calving speed control of Late-Holocene asynchronous advances and retreats, in *William O. Field Festschrift*, pp. 59–82, Univ. of Alaska Fairbanks, Fairbanks.
- Sharp, M. (1984), Annual moraine ridges at Skálafellsjökull, south-east Iceland, *J. Glaciol.*, *30*(104), 82–93.
- Truffer, M., K. A. Echelmeyer, and W. D. Harrison (2001), Implications of till deformation on glacier dynamics, *J. Glaciol.*, *47*(156), 123–134.
- van der Wateren, D. F. M. (1995), Structural geology and sedimentology of push moraines: Processes of soft sediment deformation in a glacial environment and the distribution of glaciotectionic styles, *Meded. Rijks Geolog. Dienst.*, *54*, 1–168.
- Zumberge, J. F., M. B. Heflin, D. C. Jefferson, M. M. Watkins, and F. H. Webb (1997), Precise point positioning for the efficient and robust analysis of GPS data from large networks, *J. Geophys. Res.*, *102*(B3), 5005–5018.

A. K. Bucki, ExxonMobil, 222 Benmar, Corp/GP8/720, Houston, TX 77060, USA. (acbucki@consolidated.net)

E. M. Kuriger, R. Motyka, and M. Truffer, Geophysical Institute, University of Alaska Fairbanks, 903 Koyukuk Drive, P.O. Box 757320, Fairbanks, AL 99775-7320, USA. (ekuriger@gi.alaska.edu; roman.motyka@uas.alaska.edu; truffer@gi.alaska.edu)